科技部補助專題研究計畫成果報告
期末報告

多樣式含鍶矽酸鈣於硬組織工程修復之應用研究(第2年)

計 畫 類 別 ： 個別型計畫
計 畫 編 號 ： MOST 104-2314-B-040-002-MY2
執 行 期 間 ： 105年08月01日至106年07月31日
執 行 單 位 ： 中山醫學大學牙醫學系（所）

計 畫 主 持 人： 黃翠賢
共 同 主 持 人： 高嘉澤、謝明佑
計畫參與人員： 碩士級-專任助理：黃于家

中 華 民 國 106 年 10 月 30 日

中 文 摘 要 ： 近年來的統計發現全世界約有九百萬人因為骨質疏鬆症導致相關的骨折傷害，並且在目前人口的發展速度下可以預測這一類的病人會越來越多。骨質疏鬆症是一項全身性的疾病，原因來自於體內成骨細胞與蝕骨細胞的平衡被破壞，進而導致骨密度的下降以及骨頭微結構的退化。在臨床上，這一類的病人所需要的骨頭取代物除了需具備原有可被吸收的特性外，更希望可以進一步抑制蝕骨細胞的分化。在臨床上，鍶已被證明會透過鈣離子通道來抑制成熟蝕骨細胞的分化及活性，並且已被廣泛的應用於骨質疏鬆的治療。過去本實驗室開發的矽酸鈣材料的由於降解速度太慢，導致降低其骨傳導性的特點，這會大大限制了該材料在臨床上的使用。因此，在本研究中分別利用高溫燒結法以及溶膠凝膠法來製備出含有不同鍶比例的矽酸鈣粉末，並且評估細胞培養不同成分材料上的改變。除了水泥形態的材料，在本研究中希望藉由陶瓷粉末再製備出多孔的支架，以及利用3D列印技術來製備支架已更貼近臨床使用上的便利性。另外將細胞所分泌的細胞外基質固定於支架上並進行連續性動態培養,透過細胞型態觀察、評估其生化與代謝及功能性蛋白質分子的分析,並更進一步再植入動物體內，已評估該材料在硬組織修復上應用的可行性。

中 文 關 鍵 詞 ： 矽酸鈣，鍶，3D列印支架，骨髓間葉幹細胞，骨組織工程

英 文 摘 要 ： Materials with varying degrees of bioactivity and degradation are required so as to conform to differing clinical requirements for hard tissue repair. Autograft possesses all the characteristics indispensable for new bone formation, namely, osteogenesis, osteoconductivity, and osteoinductivity, and it is currently considered the gold standard in this field. In spite of its strengths, however, there are still various disadvantages when using this material for certain medical clinical applications. Therefore, the design of an even better composite material would be very beneficial for controlling material physicochemical properties. Thus, the bone substitute materials are required to support the bone remodeling process, which consists of osteoclastic resorption and osteoblastic synthesis. Recently, several studies have indicated that calcium silicate (CS) can play an important role in bone formation, at least based upon these materials' patterns of Si ion release and its fast apatite formation ability. However, the slow degradation rate of CS may result in a decrease in osteoconductivity, which may limit its clinical application. The aim of this project was development of strontium-calcium silicate (Sr-CS) cement is potentially favorable for promoting bone regeneration and repair. The study summarizes all efforts to prepare the composite cement, and investigate their surface microstructure, bioactivity, biodegradability and in vitro cell response. In addition, the 3D printing technique could

better control the macroporous structure and mechanical property of Sr-CS scaffolds at the same time. In order to approach the resolution and pore sizes relevant for scaffold engineering were selected and compared. This study focused on optimizing the formulation of the binder solution used in room temperature 3D printing of Sr-CS for optimized accuracy, mechanical strength, and biocompatibility. It is reasonable to expect that 3D printing of Sr-CS scaffolds for bone regeneration would be promising. We hypothesize that the combination of Si and Sr in biomaterials may promote osteoporotic bone regeneration by synergistic effects to stimulate the osteogenic differentiation of mesenchymal stem cells (MSCs). In addition, the ovariectomized rat (OVX rat) calvarial defect model was used to investigate the regulatory effect of Sr-CS on the in vivo bone formation ability.

英文關鍵詞：Calcium silicate, strontium, 3D printed scaffold, bone marrow mesenchymal stem cell, bone tissue engineering

科技部補助專題研究計畫成果報告

（□期中進度報告/v 期末報告）

多樣式含鍶矽酸鈣於硬組織工程修復之應用研究

計畫類別：v 個別型計畫　□整合型計畫

計畫編號：104-2314-B-040 -002 -MY2

執行期間：201 屮/08/01～2017/07/31

執行機構及系所：中山醫學大學牙醫系

計畫主持人：黃翠賢

期末報告處理方式：

1. 公開方式：

   □非列管計畫亦不具下列情形，立即公開查詢

   □涉及專利或其他智慧財產權，□一年 v 二年後可公開查詢

2.「本研究」是否已有嚴重損及公共利益之發現：v 否 □是

3.「本報告」是否建議提供政府單位施政參考 v 否 □是，____（請列舉提供之單位；本部不經審議，依勾選逕予轉送）

中　華　民　國 106 年 10 月

Introduction

Bone grafts are required due to bone loss resulted from ablative tumor surgery or traumatic injuries. Although the autografts are ideal for bone substitution to avoid disease transmission and immunogenic rejection, synthetic bone grafts are often selected when autografts are limited or considering complications after additional surgery to harvest autologous bone graft [1]. Calcium phosphate ceramics are widely accepted bone grafting materials for bone regeneration because of their excellent osteoconductivity and mechanical properties [2]. The released calcium ions have been reported to have a significant effect on osteoblast proliferation and regulation [3]. Osteoporosis, a systemic musculoskeletal disease, occurs when bone resorption process by osteoclasts exceeded the bone formation rate by osteoblasts; results in low bone mass and micro-architectural deterioration of bone tissue [1]. Progressively, the weakened bone can increase the risk toward bone fractures. In the clinical, there were various treatment methods have been developed for osteoporosis based on either the inhibition of bone resorption by strontium ranelate (SrR) [4]. SrR has been used as additives in medicine to maintain bone strength and to prevent both vertebral and non-vertebral bone fractures in patients with osteoporosis in clinical practices. As strontium shows similar chemical and biological behavior to calcium, several reports have shown that strontium also has effects on bone metabolism, stimulating bone formation and inhibiting bone resorption when integrated with the skeleton [5].

Calcium silicate (CS)-based ceramic exhibits eminent biocompatibility, bioactivity and biodegradability [6-8]. CS-based materials were referred as mineral trioxide aggregate (MTA) cement in dentistry, have been used as filling-sealing materials in root canal treatment and shown great clinical results [9,10]. Recently, CS-based biomaterials have been the choice over the traditional calcium phosphate bioceramics for bone substitute and regeneration applications, which was attributed to its ability to induce formation of a bone-like apatite and promote early

bone growth [11]. In addition, CS based biomaterial has shown antibacterial properties because of the alkaline property [12]. Due to nature of ceramic material, poor mechanical properties have made CS non-applicable under load-bearing situation. In order to increase CS physical properties, CS composite containing ZnO, MgO, Fe_2O_3 have been explored by researchers [11,13]. Feng et al. have developed CS composite with addition of hydroxyapatite (HA) fibrous materials to increase the mechanical strength. The mechanical properties were increased but not comparable to those of cortical bone. In addition, the degradation rate of bone substitute is crucial and should match the new bone tissue formation during remodeling. Therefore, a CS and tricalcium phosphate composite with controlled degradation has been developed [14].

Since calcium can be substitute by strontium due to their similarity in charge and ionic radius, several approaches incorporated with strontium have reported using substitution or doping of biomaterials such as natural bone powder, polycaprolactone composite, bioactive glasses/ceramics and hydroxyapatite for bone regeneration applications [15-17]. The addition of strontium in bone cement or scaffold has shown great potential for increasing the effectiveness of bone remodeling and regeneration in the early stage of implantation. Zhang et al demonstrated that doping Sr into bioglass 3D scaffolds is a hopeful and effective method to form tissue engineering scaffolds in combination with the bioactivity of bioglass and the anti-osteoporotic effect of Sr ion [18]. The Sr-contained calcium phosphate cement indicated excellent properties of setting time, compressive strength, and radiopacity [19]. The composites stimulated the adhesion and osteogenesis of human mesenchymal stem cells and promoted new bone regeneration at the bone−materials interface [19].

In this study, we therefore doped Sr into the synthesized CS ceramic with a mixture of PCL for establishing a 3D scaffold by using a 3D printing system for the mandible of the ovariectomized rat with induction of periodontal disease. The resulting 3D printed scaffolds on material characterization and cellular interactions were quantitative measured. In addition,

improvement of osteoporosis was further evaluated histologically. The results of this study may lead to better treatment of dental osteopenia patients.

2. Materials and Methods

2.1. Sr-CS powder preparation

The method used here for the preparation of Sr-CS powder has been described elsewhere [20]. In brief, reagent grade SiO_2 (High Pure Chemicals, Saitama, Japan), CaO (Sigma-Aldrich, St. Louis, MO), and MgO (Sigma-Aldrich) powders were used as matrix materials (composition: 75% CaO + SrO, and 25% SiO_2). The nominal weight ratios of CaO-SiO2–SrO are listed in Table 1. The oxide mixtures were then sintered at 1,400°C for 2 h using a high-temperature furnace and then ball-milled in ethyl alcohol using a centrifugal ball mill (S 100, Retsch, Hann, Germany) for 6 h. The sintered powder was mixed using a liquid/powder ratio of 0.35 mL/g. After being mixed with water, the cements were molded in a Teflod mold (diameter: 6 mm, height: 3 mm). There was enough cement to fully cover each well of the 24-well plate (GeneDireX, Las Vegas, NV) to a thickness of 2 mm for in vivo test. All specimens were stored in an incubator at 100% relative humidity and 37°C for 1 day of hydration.

2.2. Preparation of the Sr-CS/PCL paste

Sr-CS powder was immersed in 99.5% ethanol and stirred at 400 rpm overnight. The homogenously dissolved CS in ethanol was slowly added into molten PCL beads (Mw = 43000–50000, Polysciences, Warrington, PA) and stirred with a metal rod at 200°C until the CS-ethanol solution was evenly mixed with the PCL to create a Sr-CS/PCL paste. After mixing, the paste was left in the oven at 85˚C for 1 day.

2.3. Scaffold fabrication

The Sr-CS/PCL 3D scaffolds were manufactured with a BioScaffolder (BioScaffolder 3.1, GeSiM, Großerkmannsdorf, Germany). The CS/PCL paste was transferred into the printing cartridge with a 20G nozzle. The printing speed was 2 mm/s under 450 kPa of extrusion pressure. The 3D-scaffold measured 6.5 mm X 6.5 mm X 10.0 mm. After printing, the scaffold was allowed to dry at room temperature for 2h. The strut with a diameter of 500 μm were printed in parallel with a gap of 500 μm between the struts. Subsequent layers were printed at an angle of 90º with the underlying layer. The scaffolds were then irradiated with a dental CO_2 laser with an output of 10600 nm (Opelaser Pro, Yoshida Co. Ltd, Tokyo, Japan) using directly mounted fiber optics in would healing mode with a spot area of 0.25 cm^2, and stored in an incubator at 100% relative humidity and 37 °C for 1 day to set.

2.4. Characterization

The water contact angle for each scaffold was considered at room temperature. Briefly, the scaffolds were placed on the top of a stainless-steel base; a drop of 20 μL Dulbecco's modified Eagle medium (DMEM; Caisson, North Logan, UT, USA) was placed on the surface of the scaffolds, and an image was taken with a camera after 20 min had elapsed. The resulting images were analyzed using ImageJ (National Institutes of Health) to determine the water contact angle. The phase composition of the cements was analyzed using X-ray diffractometry (XRD; Bruker D8 SSS, Karlsruhe, Germany), run at 30 kV and 30 mA at a scanning speed of 1o/min. The morphology of the cement specimens was coated with gold and examined under a scanning electron microscope (SEM; JSM-6700F, JEOL) operated in the lower secondary electron image (LEI) mode at 3 kV accelerating voltage. Finally, the compressive strength of the scaffolds was measured on an EZ-Test machine (Shimadzu, Kyoto, Japan) at a loading rate of 1 mm/min. The maximum compressive load at failure was obtained from the recorded load-

deflection curves. Three independent measurements were carried out and the data were expressed as mean ± SD.

2.5. In vitro soaking

The bioactivities of the Sr-CS scaffolds were evaluated by examining the formation of bone-like apatite on the samples in simulated body fluid (SBF) solution. The Sr-CS samples with a thickness of 3 mm and a diameter of 6 mm were immersed in 10 mL SBF at 37°C in a humidified atmosphere for various time-points. Then, the Sr-CS materials were gently rinsed with ddH2O to remove SBF and dried at 80°C. The surfaces of the immersed samples were observed by SEM. The Ca, Si, Sr, and P ions concentration released from specimens on SBF were considered by an inductively coupled plasma-atomic emission spectrometer (ICP-AES; Perkin-Elmer OPT 1MA 3000DV, Shelton, CT, USA). In addition, the degradation of specimens was determined by monitoring the weight change following immersion in a SBF. After drying at 100^{o}C for 1 day, the Sr-CS cements were weighed both before and after immersion by a balance (TE214S, Sartorius, Goetingen, Germany). Ten samples were measured for each of the specimens investigated at each time point. In addition, the pH value measurement was considered before and after specimens soaking.

2.6. Cell proliferation

Before performing the cell experiments, all scaffolds were sterilized by being immersed in 75% ethanol and exposed to ultraviolet light for 15 min. The human Wharton's Jelly mesenchymal stem cells (WJMSCs) were obtained from the Bioresource Collection and Research Center (BCRC, Hsin-Chu, Taiwan) and grown in a mesenchymal stem cell medium (Sciencell) to passage 3–6. The WJMSCs were directly cultured on the scaffolds at a density of 5x10^{4} cells per well in a DMEM-filled 48-well plate and incubated at 37°C in a 5% CO_2

atmosphere for various durations. After different culturing, the cell viability was considered using the PrestoBlue® (Invitrogen, Grand Island, NY) assay. At the end of the culture period, the DMEM was removed, and the wells were washed twice with cold PBS. Then, each well with a specimen was filled with PrestoBlue® and fresh DMEM at a ratio of 1:9 and incubated at 37°C for 60 min. The resulting solution in each well was then transferred to a new 96-well plate, and the optical density (OD) of the solutions was measured using Tecan Infinite 200® PRO microplate reader (Tecan, Männedorf, Switzerland) at 570 nm with a reference wavelength of 600 nm. The results were obtained in triplicate from three separate experiments. The cell cultured on tissue culture plates without scaffolds were used as a control (Ctl).

2.7. Osteogenesis and angiogenesis assay

In this study, we consider the osteogenic-, and angiogenic-related genes (ALP, OPN, OC, vWF and Ang-1), of hMSCs after being cultured for 7 days. Total RNA of all five groups was extracted using TRIzol reagent (Invitrogen) and analyzed using RT-qPCR. Total RNA (500 ng) was used for the synthesis of complementary DNA using a cDNA Synthesis Kit (GeneDireX) following the manufacturer's instructions. RT-qPCR primers (Table 1) were designed based on cDNA sequences from the NCBI Sequence database. SYBR Green qPCR Master Mix (Invitrogen) was used for detection and the target mRNA expressions were assayed on the ABI Step One Plus real-time PCR system (Applied Biosystems, Foster City, California, USA). Each sample was performed in triplicate.

2.9. Animal

The accumulated calcium deposition on the WJMSCs after 2 and 3 weeks of culturing in osteogenic differentiation medium was analyzed using Alizarin Red S staining, as developed in a previous study [12]. In brief, the specimens were fixed with 4% paraformaldehyde (Sigma-

Aldrich) for 15 min and then incubated in 0.5% Alizarin Red S (Sigma-Aldrich) at a pH of 4.0 for 15 min at room temperature. After this, the cells were washed with PBS and photographs were taken using an optical microscope (BH2-UMA, Olympus, Tokyo, Japan) equipped with a digital camera (Nikon, Tokyo, Japan) at a 200x magnification. The Alizarin Red was also quantified using a solution of 20% methanol and 10% acetic acid in water. After 15 min, the liquid was transferred to a 96-well, and the quantity of Alizarin Red was determined using a spectrophotometer at 450 nm.

2.10. Statistical Analysis

A one-way analysis of the variance statistical data was used to evaluate the significance of the differences between the means in the measured data. A Scheffe's multiple comparison test was used to determine the significance of the deviations in the data for each specimen. In all cases, the results were considered statistically significant with a p value < 0.05.

3. Results and discussion

3.1. The characterization of CS/PCL scaffolds

A layer-by-layer plotted Sr-CS/PCL scaffold in which 10%, 30%, and 50% CS mixed with PCL was fabricated. The scaffold showed a fully interconnected, well-defined pore morphology and porous structure. Photographs of the printed Sr-CS/PCL hybrid 3D-scaffold are shown in Fig. 1. The parameter of 3D-scaffolds was measured by 6.5 mm X 6.5 mm X 10.0 mm. When the content of Sr-CS is increased, the colour of the scaffold will gradually be yellowed from the original PCL white. The hydrophilic behavior of Sr-CS/PCL scaffolds were tested by measuring the contact angle as shown in Fig. 2. The effect of contact angle on the measurement time was tested by contacting the DMEM droplet for 20 minutes at room temperature. The time-dependent contact

angles of Sr0, Sr5, and Sr10 scaffold were measured. The contact angles have slightly decreased in each specimen within 20 minutes after deposition. The contact angle of prepared CS/PCL scaffolds could be decreased from 65.8 ± 3.2^{o}, 63.7 ± 2.6 ^{o}, and 59.8 ± 3.4^{o} with Sr0, Sr5, and Sr10, respectively.

XRD patterns of CS/PCL composite scaffolds at various weight ratios are demonstrated in Fig. 3. These main characteristic peaks gradually decreased with the percentage of CS content increasing. Instead, the intensity of the diffraction peak of Sr-CS was found approximately at the range of 2θ from 29° to 34° [12]. CS50 has an obvious diffraction peak near 2θ = 29.4°, which corresponds to the CSH gel, and incompletely reacted inorganic component phases of the β-dicalcium silicate (β-Ca2SiO4) at 2θ between 32° and 34° [2]. Fig. 4 shows the stress–strain curve for the different ratio of Sr-CS/PCL hybrid scaffolds with dimensions of 6 mm x 6 mm x 10 mm at a constant stretching velocity of 0.5 mm/sec until deformation up to 20%. With increased in the amount of Sr, the compressive strength of composite scaffold appeared significantly superior to those with the relatively lower proportion of Sr, but the brittle behavior of scaffold also increased due to the inherently poor tensile strength of Sr0. We supposed the increase in mechanical properties of the Sr-CS/PCL composites scaffolds, compared to PCL, can be attributed to the formation of Sr-CS agglomerates, which may result in the homogeneous dispersion of the inorganic filler into the PCL materials [24].

3.2. Bioactivity

SEM was utilized to analyze the morphology and microstructure of the 3D scaffolds. The images of the scaffolds' surface before and after immersion in SBF for 7 days were shown in Fig. 5. As can be seen, the Sr0 retained a smooth and dense surface during the soaking time-

points. On the contrary, the scaffold with Sr-CS contained had affection for it after immersion for 1 day in SBF, miniature globular particles were spread all over the surfaces which were formed of apatite precipitates. The precipitated of the bone-like apatite on scaffold surface has proven to be useful in predicting the bone-bonding behavior of bone substitutes in vitro [8]. There were few apatite spheres precipitate on Sr0, Sr5, and Sr10 surface with an average size of less than 1 μm after immersed for day. However, Sr10 was uniformly covered with spherical aggregated minerals. As reported in a previous study [26-28], Ca ions released from CS-based substrates possibly originating from the less-ordered hydration products that promoted significantly apatite growth by increasing local Ca concentration, thereby raising the ionic product of the apatite in the surrounding environment and enhancing the nucleation behavior of the apatite [29]. The apatite formation on the CS-based scaffolds surface contained release of Ca ion from the scaffolds and the Si-OH hydrate supplied favourable sites for apatite nucleation [30]. The main phenomenon could be attributed to the accessibility nucleation sites for the silicates. When the soaking time reached to day 7, sustained formation of covered apatite layers was getting thicker, especially in the specimen of Sr10.

3.4. Cell proliferation

The proliferation of WJMSC shown in Fig. 6 indicates that adhered cell on the 3D scaffolds were more than 90% of Ctl in the first 6 h. Still, with increasing the concentration of Sr, the cell proliferation and viability was higher than that on Sr0 and the Ctl, indicating that Sr could be used as a promising bioactive material to enhance biocompatibility. The cell adhesion ability can be inhibited if cultured on material with hydrophobic, while a scaffold contained CS are extremely hydrophilic [20]. After 1 day of culture, the quantitative analysis showed that the proliferation of WJMSC cultured on Sr10 was significantly higher than that of the Sr0 (1.16 fold) and Sr5 (1.05 fold) groups. The stimulatory and dose-dependent

proliferation effects of Si and Sr ionic products have been well-proven in various studies [8]. Shie et al. reported that the ion concentration of Si of 1 mM in cell culture medium increased the proliferation of osteoblast-like cell [37]. Hence, we suggested the Si and Sr ions with certain concentration released from Sr5 and Sr10 scaffolds enhanced the adhesion and proliferation of WJMSC cells. The results of the undecalcified samples stained with Van Kossa's staining (Fig. 8) show that the newly formed bone into the Sr10 group was mainly detected in the periphery of the defect at week 4 after operation.

4. Conclusions

In this work, we have demonstrated the novel Sr-CS-based material blended with PCL was developed by the solvent-free processing to conquer the limitation of biological behavior and fabricated the ideal porous 3D scaffold with adequate pore morphology and pore size for bone tissue engineering. Our results demonstrate that the 3D Sr-CS scaffold not only increases in mechanical properties but also provide suitable highly hydrated tissue-like microenvironments to support hMSCs adhesion and proliferation. Moreover, osteogenic and angiogenesis differentiation of hMSCs were further highly improved, thus making them emerging for regenerative medicine applications in the future. Our results would assist the fabricated of 3D scaffolds with increased bioceramic leading to more robust or greater range of biological behaviours.

Reference

[1] X. Shen, P. Ma, Y. Hu, G. Xu, K. Xu, W. Chen, et al., Alendronate-loaded hydroxyapatite-TiO2 nanotubes for improved bone formation in osteoporotic rabbits, J Mater Chem B. 4 (2016) 1423–1436.

[2] M.H. Huang, C.T. Kao, Y.W. Chen, T.T. Hsu, D.E. Shieh, T.H. Huang, et al., The synergistic effects of chinese herb and injectable calcium silicate/b-tricalcium phosphate composite on an osteogenic accelerator in vitro, J Mater Sci: Mater Med. 26 (2015) 161.

[3] G.Y. Jung, Y.J. Park, J.S. Han, Effects of HA released calcium ion on osteoblast differentiation, J Mater Sci: Mater Med. 21 (2010) 1649–1654.

[4] E. Bonnelye, A. Chabadel, F. Saltel, P. Jurdic, Dual effect of strontium ranelate: stimulation of osteoblast differentiation and inhibition of osteoclast formation and resorption in vitro, Bone. 42 (2008) 129–138.
[5] E. Boanini, P. Torricelli, M. Gazzano, E. Della Bella, M. Fini, A. Bigi, Combined effect of strontium and zoledronate on hydroxyapatite structure and bone cell responses, Biomaterials. 35 (2014) 5619–5626.
[6] L. Zhang, X. Huang, Y. Han, Formation mechanism and cytocompatibility of nano-shaped calcium silicate hydrate/calcium titanium silicate/TiO2 composite coatings on titanium, J Mater Chem B. 4 (2016) 6734–6745.
[7] F. Costa, P. Sousa Gomes, M.H. Fernandes, Osteogenic and angiogenic response to calcium silicate-based endodontic sealers, J Endod. 42 (2016) 113–119.
[8] Y.W. Chen, T.T. Hsu, K. Wang, M.Y. Shie, Preparation of the fast setting and degrading Ca-Si-Mg cement with both odontogenesis and angiogenesis differentiation of human periodontal ligament cells, Mater Sci Eng C Mater Biol Appl. 60 (2016) 374–383.
[9] Y.W. Chen, C.C. Ho, T.H. Huang, T.T. Hsu, M.Y. Shie, The ionic products from mineral trioxide aggregate–induced odontogenic differentiation of dental pulp cells via activation of the Wnt/β-catenin signaling pathway, J Endod. 42 (2016) 1062–1069.
[10] S.E. Yoldaş, M. Bani, D. Atabek, H. Bodur, Comparison of the potential discoloration effect of bioaggregate, biodentine, and white mineral trioxide aggregate on bovine teeth: In vitro research, J Endod. 42 (2016) 1815–1818.
[11] Y.W. Chen, C.H. Yeh, M.Y. Shie, Stimulatory effects of the fast setting and degradable Ca–Si–Mg cement on both cementogenesis and angiogenesis differentiation of human periodontal ligament cells, J Mater Chem B. 3 (2015) 7099–7108.
[12] M.H. Huang, Y.F. Shen, T.T. Hsu, T.H. Huang, M.Y. Shie, Physical characteristics, antimicrobial and odontogenesis potentials of calcium silicate cement containing hinokitiol, Mater Sci Eng C Mater Biol Appl. 65 (2016) 1–8.
[13] D. Bellucci, A. Sola, A. Anesi, R. Salvatori, L. Chiarini, V. Cannillo, Bioactive glass/hydroxyapatite composites: mechanical properties and biological evaluation, Mater Sci Eng C Mater Biol Appl. 51 (2015) 196–205.
[14] C.T. Kao, T.H. Huang, Y.J. Chen, C.J. Hung, C.C. Lin, M.Y. Shie, Using calcium silicate to regulate the physicochemical and biological properties when using β-tricalcium phosphate as bone cement, Mater Sci Eng C Mater Biol Appl. 43 (2014) 126–134.
[15] W. Zhang, F. Zhao, D. Huang, X. Fu, X. Li, X. Chen, Strontium-substituted submicrometer bioactive glasses modulate macrophage responses for improved bone regeneration, ACS Appl Mater Interfaces. 8 (2016) 30747–30758.
[16] Ł. John, M. Podgórska, J.-M. Nedelec, Ł. Cwynar-Zając, P. Dzięgiel, Strontium-doped organic-inorganic hybrids towards three-dimensional scaffolds for osteogenic cells, Mater Sci Eng C Mater Biol Appl. 68 (2016) 117–127.
[17] H. Zhu, D. Zhai, C. Lin, Y. Zhang, Z. Huan, J. Chang, et al., 3D plotting of highly uniform $Sr_5(PO_4)_2SiO_4$ bioceramic scaffolds for bone tissue engineering, J Mater Chem B. 4 (2016) 6200–6212.
[18] Y. Zhang, L. Wei, J. Chang, R.J. Miron, B. Shi, S. Yi, et al., Strontium-incorporated mesoporous bioactive glass scaffolds stimulating in vitro proliferation and differentiation of bone marrow stromal cells and in vivo regeneration of osteoporotic bone defects, J Mater Chem B. 1 (2013) 5711–5722.

[19] Y. Zhang, X. Cui, S. Zhao, H.C. Wang, M.N. Rahaman, Z. Liu, et al., Evaluation of injectable strontium-containing borate bioactive glass cement with enhanced osteogenic capacity in a critical-sized rabbit femoral condyle defect model, ACS Appl Mater Interfaces. 7 (2015) 2393–2403.
[20] Y.L. Cheng, Y.W. Chen, K. Wang, M.Y. Shie, Enhanced adhesion and differentiation of human mesenchymal stem cell inside apatite-mineralized/poly(dopamine)-coated poly(ε-caprolactone) scaffolds by stereolithography, J Mater Chem B. 4 (2016) 6307–6315.
[21] K.Y. Tsai, H.Y. Lin, Y.W. Chen, C.Y. Lin, T.T. Hsu, C.T. Kao, Laser sintered magnesium-calcium silicate/poly-ε-caprolactone scaffold for bone tissue engineering, Materials. 10 (2017) 65.
[22] S.H. Huang, T.T. Hsu, T.H. Huang, C.Y. Lin, M.Y. Shie, Fabrication and characterization of polycaprolactone and tricalcium phosphate composites for tissue engineering applications, J Dent Sci. 12 (2017) 33–43.
[23] F.C. Kung, C.C. Lin, W.F.T. Lai, Osteogenesis of human adipose-derived stem cells on hydroxyapatite-mineralized poly(lactic acid) nanofiber sheets, Mater Sci Eng C Mater Biol Appl. 45 (2014) 578–588.
[24] K.K. Gómez-Lizárraga, C. Flores-Morales, M.L. Del Prado-Audelo, M.A. Álvarez-Pérez, M.C. Piña-Barba, C. Escobedo, Polycaprolactone- and polycaprolactone/ceramic-based 3D-bioplotted porous scaffolds for bone regeneration: A comparative study, Mater Sci Eng C Mater Biol Appl. 79 (2017) 326–335.
[25] A. Mohammadkhah, L.M. Marquardt, S.E. Sakiyama-Elbert, D.E. Day, A.B. Harkins, Fabrication and characterization of poly-(ε)-caprolactone and bioactive glass composites for tissue engineering applications, Mater Sci Eng C Mater Biol Appl. 49 (2015) 632–639. doi:10.1016/j.msec.2015.01.060.
[26] M. Mehrali, E. Moghaddam, S.F.S. Shirazi, S. Baradaran, M. Mehrali, S.T. Latibari, et al., Synthesis, mechanical properties, and in vitro biocompatibility with osteoblasts of calcium silicate-reduced graphene oxide composites, ACS Appl Mater Interfaces. 6 (2014) 3947–3962.
[27] C.H. Liu, T.H. Huang, C.J. Hung, W.Y. Lai, C.T. Kao, M.Y. Shie, The synergistic effects of fibroblast growth factor-2 and mineral trioxide aggregate on an osteogenic accelerator in vitro, Int Endod J. 47 (2014) 843–853.
[28] D.C. Zancanela, A.N. de Faria, A.M.S. Simão, R.R. Gonçalves, A.P. Ramos, P. Ciancaglini, Multi and single walled carbon nanotubes: effects on cell responses and biomineralization of osteoblasts cultures, J Mater Sci: Mater Med. 27 (2016) 62.
[29] C.C. Ho, H.Y. Fang, B. Wang, T.H. Huang, M.Y. Shie, The effects of Biodentine/polycaprolactone 3D-scaffold with odontogenesis properties on human dental pulp cells, Int Endod J. (2017). doi:10.1111/iej.12799.
[30] X. Liu, C. Ding, P.K. Chu, Mechanism of apatite formation on wollastonite coatings in simulated body fluids, Biomaterials. 25 (2004) 1755–1761.
[31] W.Y. Lai, Y.W. Chen, C.T. Kao, T.T. Hsu, T.H. Huang, M.Y. Shie, Human dental pulp cells responses to apatite precipitation from dicalcium silicates, Materials. 8 (2015) 4491–4504.
[32] M.Y. Shie, W.H. Chiang, I.W.P. Chen, W.Y. Liu, Y.W. Chen, Synergistic acceleration in the osteogenic and angiogenic differentiation of human mesenchymal stem cells by calcium silicate–graphene composites, Mater Sci Eng C Mater Biol Appl. 73 (2017) 726–735.

[33] C.J. Su, M.G. Tu, L.J. Wei, T.T. Hsu, C.T. Kao, T.H. Chen, et al., Calcium silicate/chitosan-coated electrospun poly (lactic acid) fibers for bone tissue engineering, Materials. 10 (2017) 501.
[34] C.Y. Huang, T.H. Huang, C.T. Kao, Y.H. Wu, W.C. Chen, M.Y. Shie, Mesoporous calcium silicate nanoparticles with drug delivery and odontogenesis properties, J Endod. 43 (2017) 69–76.
[35] E. Abed, R. Moreau, Importance of melastatin-like transient receptor potential 7 and magnesium in the stimulation of osteoblast proliferation and migration by platelet-derived growth factor, Am J Physiol Cell Physiol. 297 (2009) C360–C368.
[36] R. Jugdaohsingh, L.D. Pedro, A. Watson, J.J. Powell, Silicon and boron differ in their localization and loading in bone, Bone Reports. 1 (2015) 9–15.
[37] M.Y. Shie, S.J. Ding, H.C. Chang, The role of silicon in osteoblast-like cell proliferation and apoptosis, Acta Biomater. 7 (2011) 2604–2614. doi:10.1016/j.actbio.2011.02.023.
[38] Z. Gu, S. Wang, W. Weng, X. Chen, L. Cao, J. Wei, et al., Influences of doping mesoporous magnesium silicate on water absorption, drug release, degradability, apatite-mineralization and primary cells responses to calcium sulfate based bone cements, Mater Sci Eng C Mater Biol Appl. 75 (2017) 620–628.
[39] M.Y. Shie, S.J. Ding, Integrin binding and MAPK signal pathways in primary cell responses to surface chemistry of calcium silicate cements, Biomaterials. 34 (2013) 6589–6606.
[40] L. Mao, L. Xia, J. Chang, J. Liu, L. Jiang, C. Wu, The synergistic effects of Sr and Si bioactive ions on osteogenesis, osteoclastogenesis and angiogenesis for osteoporotic bone regeneration, Acta Biomater. 61 (2017) 217–232.
[41] L.J. Fuh, Y.-J. Huang, W.C. Chen, D.J. Lin, Preparation of micro-porous bioceramic containing silicon-substituted hydroxyapatite and beta-tricalcium phosphate, Mater Sci Eng C Mater Biol Appl. 75 (2017) 798–806.
[42] E. Rathinam, S. Rajasekharan, R.T. Chitturi, H. Declercq, L. Martens, P. De Coster, Gene expression profiling and molecular signaling of various cells in response to tricalcium silicate cements: A systematic review, J Endod. 42 (2016) 1713–1725.

Figure Legends

Figure 1. The photographs of top view and side view of different various Sr-CS/PCL scaffold.

Figure 2. Water contact angle of different various Sr-CS/PCL scaffold.

Figure 3. XRD patterns of the various Sr-CS/PCL scaffolds.

Figure 4. The strain-stress curves of different Sr-CS/PCL scaffolds.

Figure 5. Surface SEM images of the Sr-CS/PCL scaffolds before and after immersion in SBF.

Figure 6. Proliferation of WJMSC cultured on Sr-CS/PCL scaffolds for different time points. "*" indicates a significant difference ($p < 0.05$) compared to CS0.

Figure 7. The SEM of WJMSC cultured on Sr-CS/PCL scaffolds for 3 h, 3 days, and 7 days.

Figure 8. Von Kossa staining of scaffold after implant in rat for 8 weeks.

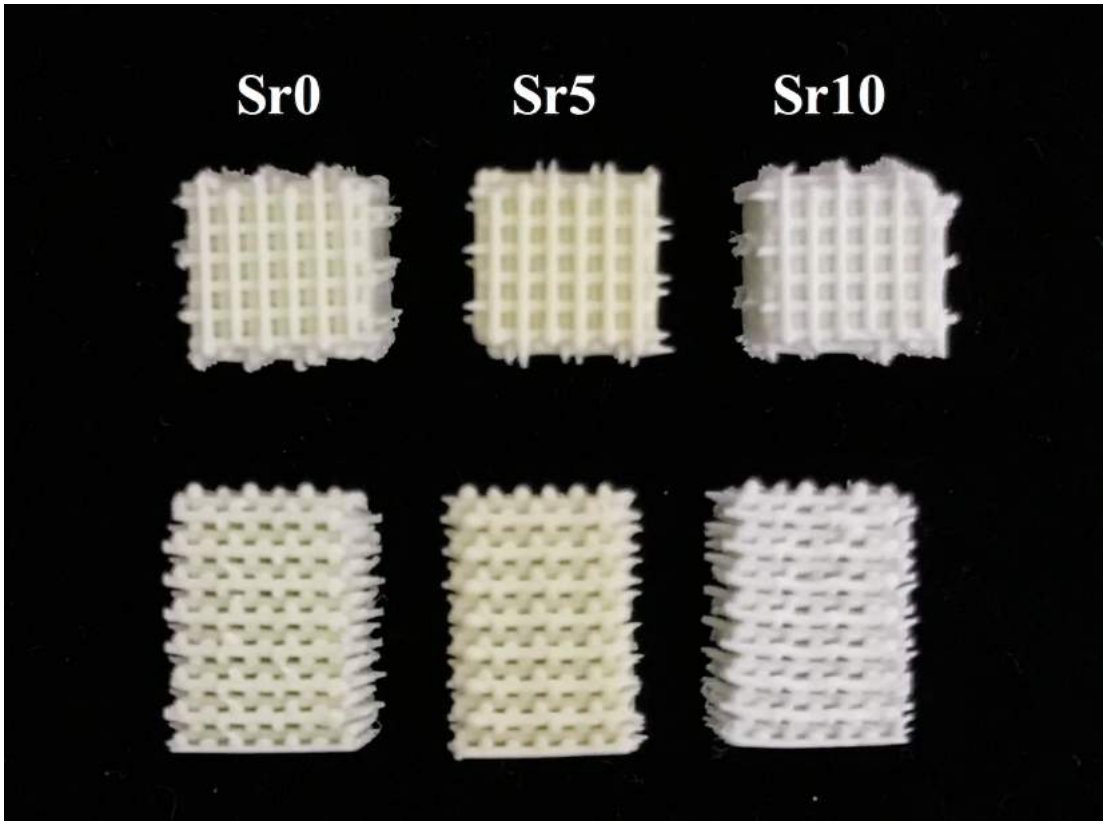

Fig 1.

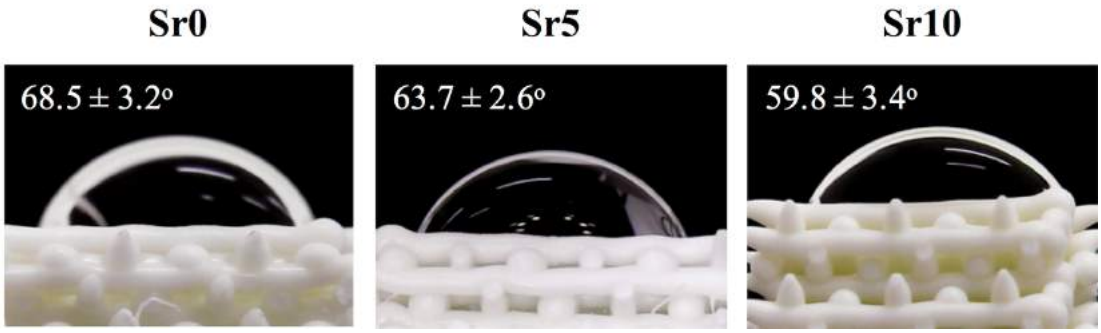

Fig 2.

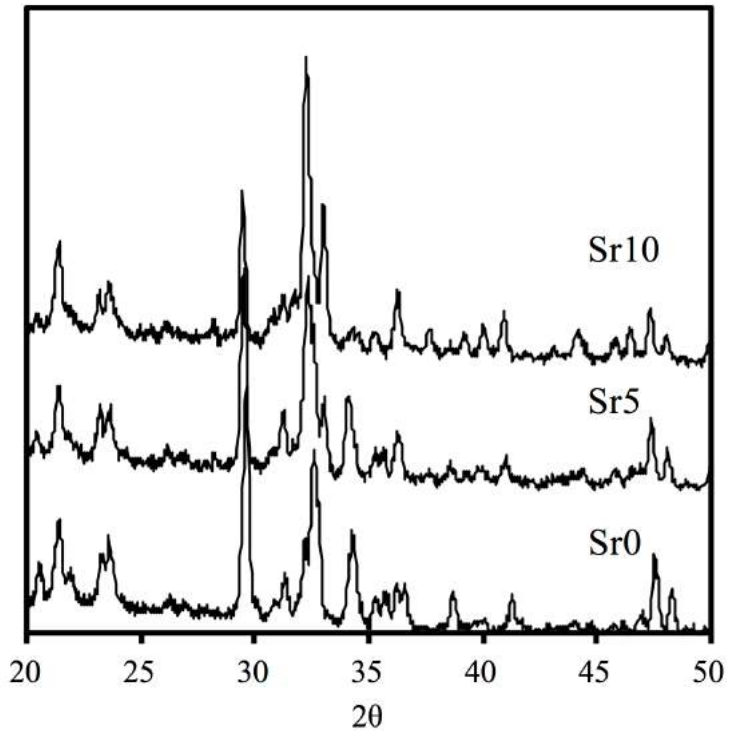
Sr10
Sr5
Sr0
20
25
30
35
40
45
50
2θ

Fig 3.

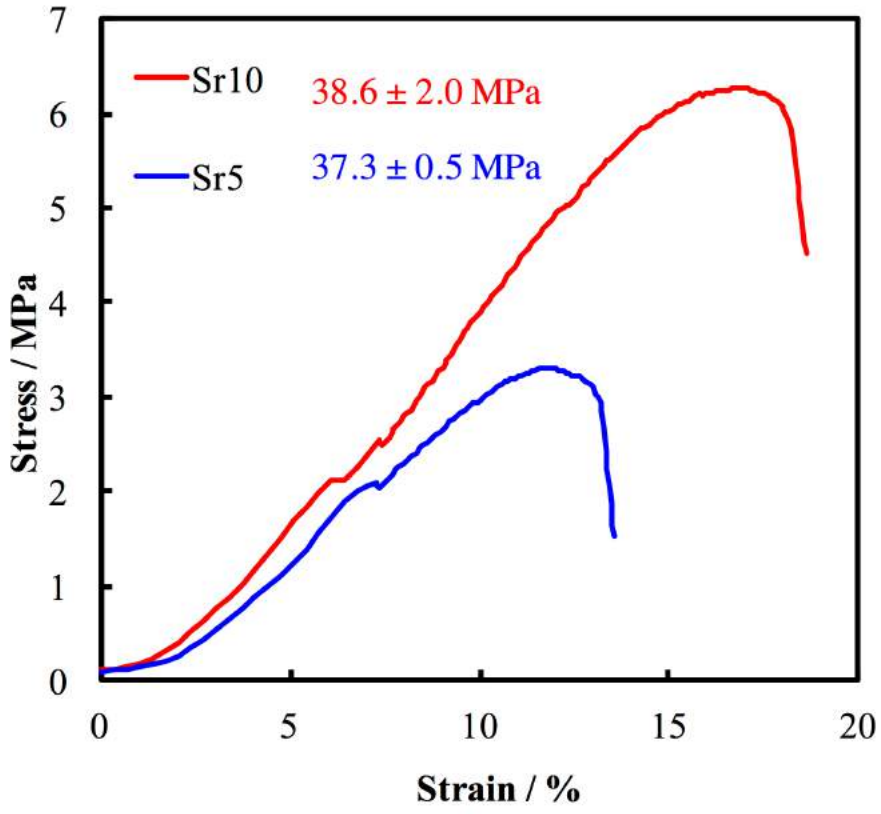
Sr10
38.6 ± 2.0 MPa
Sr5
37.3 ± 0.5 MPa
Stress / MPa
Strain / %
0
1
2
3
4
5
6
7
0
5
10
15
20

Fig 4.

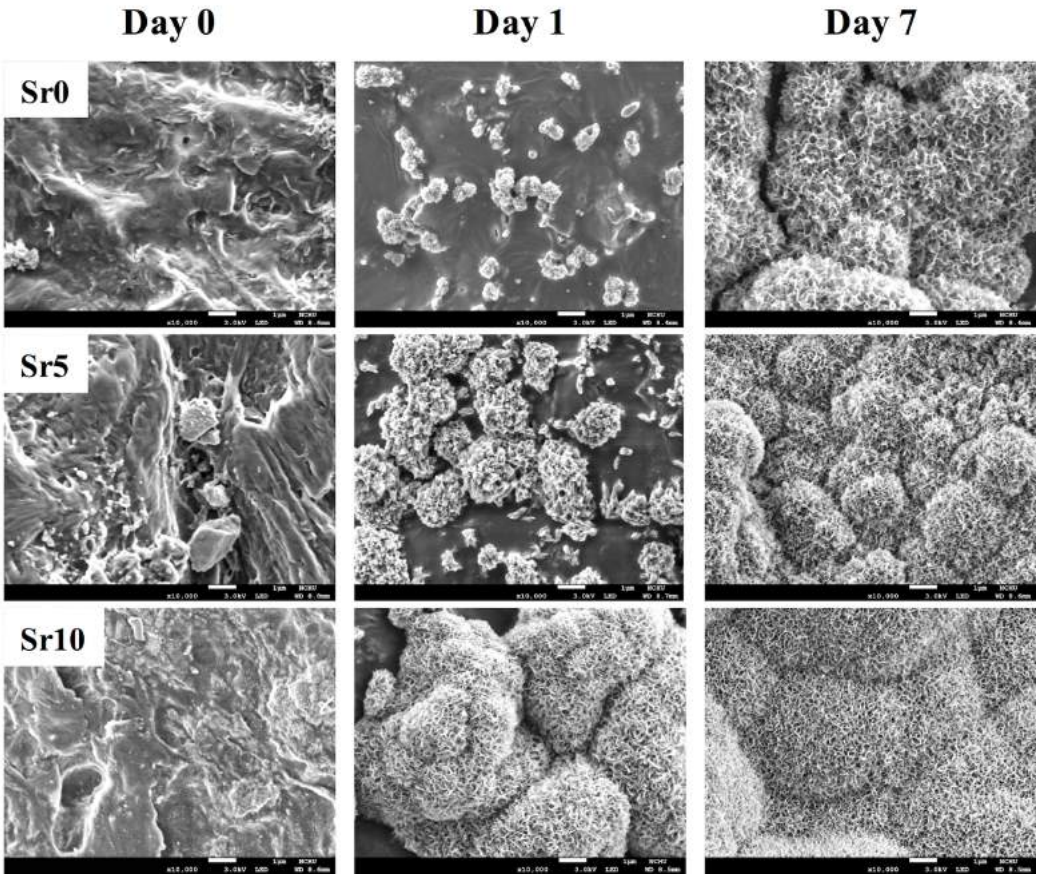
Day 0
Day 1
Day 7
Sr0
Sr5
Sr10

Fig 5.

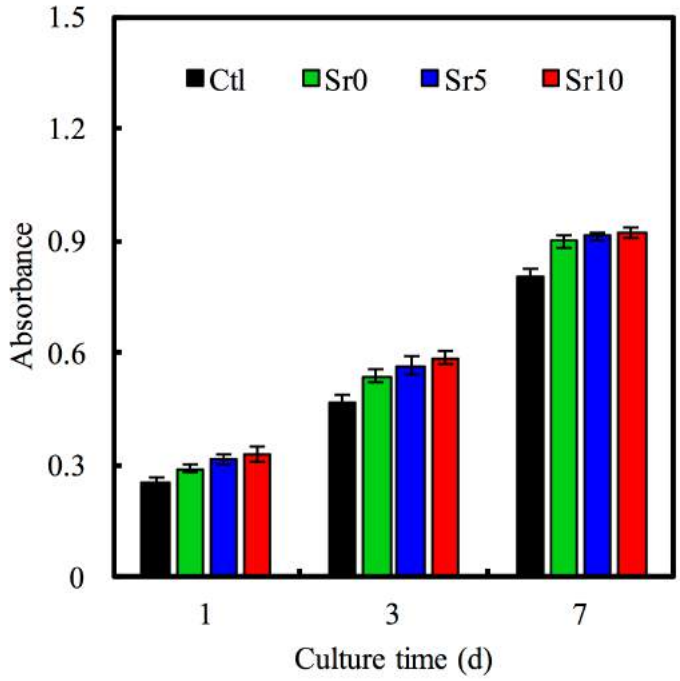
Ctl
Sr0
Sr5
Sr10
Absorbance
1.5
1.2
0.9
0.6
0.3
0
1
3
7
Culture time (d)

Fig 6.

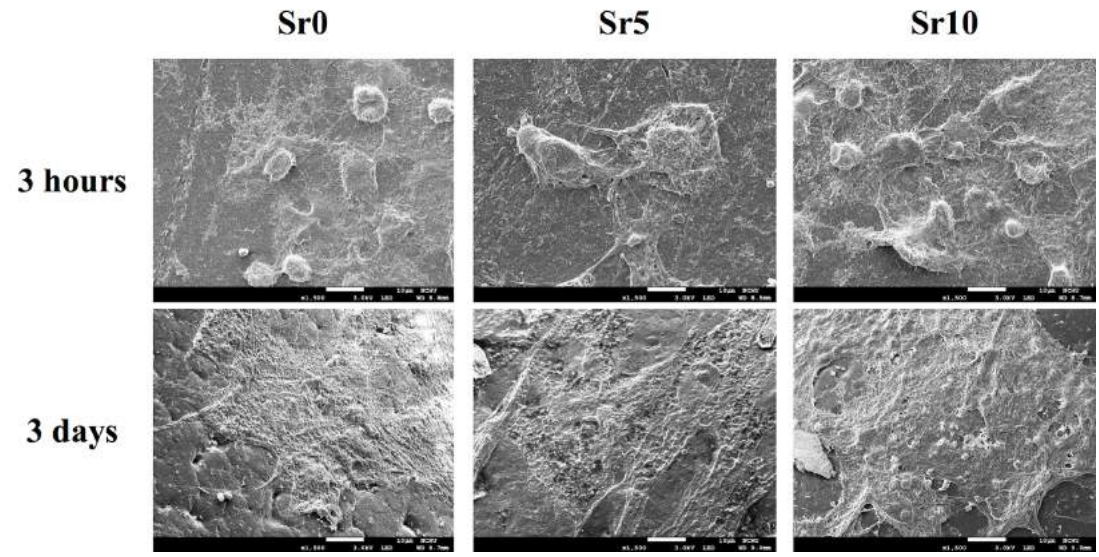

Fig 7.

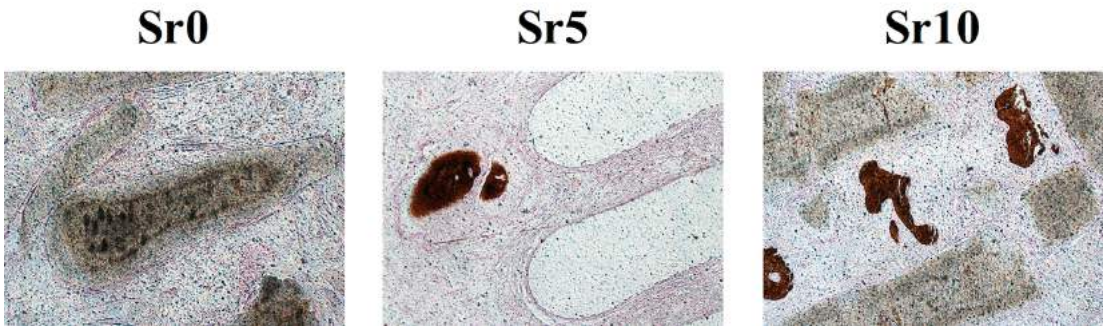

Fig 8.

104年度專題研究計畫成果彙整表

計畫主持人：黃翠賢						**計畫編號：**104-2314-B-040-002-MY2	
計畫名稱：多樣式含鍶矽酸鈣於硬組織工程修復之應用研究							
成果項目						量化	單位	質化 （說明：各成果項目請附佐證資料或細項說明，如期刊名稱、年份、卷期、起訖頁數、證號...等）
國內	學術性論文	期刊論文				0	篇	
		研討會論文				0		
		專書				0	本	
		專書論文				0	章	
		技術報告				0	篇	
		其他				0	篇	
	智慧財產權及成果	專利權	發明專利	申請中		0	件	
				已獲得		0		
			新型/設計專利			0		
		商標權				0		
		營業秘密				0		
		積體電路電路布局權				0		
		著作權				0		
		品種權				0		
		其他				0		
	技術移轉	件數				0	件	
		收入				0	千元	
國外	學術性論文	期刊論文				2	篇	Materials Science and Engineering: C 2016;65:1-8. Journal of Dental Sciences 2017;12:33-43
		研討會論文				1		2015 IADR General Session & Exhibition, Boston, USA, Mar 11－14, 2015
		專書				0	本	
		專書論文				0	章	
		技術報告				0	篇	
		其他				0	篇	
	智慧財產權及成果	專利權	發明專利	申請中		0	件	
				已獲得		0		
			新型/設計專利			0		
		商標權				0		
		營業秘密				0		

		積體電路電路布局權	0		
		著作權	0		
		品種權	0		
		其他	0		
	技術移轉	件數	0	件	
		收入	0	千元	
參與計畫人力	本國籍	大專生	0	人次	
		碩士生	1		劉孟杰
		博士生	0		
		博士後研究員	0		
		專任助理	1		黃于家
	非本國籍	大專生	0		
		碩士生	0		
		博士生	0		
		博士後研究員	0		
		專任助理	0		
其他成果 （無法以量化表達之成果如辦理學術活動、獲得獎項、重要國際合作、研究成果國際影響力及其他協助產業技術發展之具體效益事項等，請以文字敘述填列。）					

科技部補助專題研究計畫成果自評表

請就研究內容與原計畫相符程度、達成預期目標情況、研究成果之學術或應用價值（簡要敘述成果所代表之意義、價值、影響或進一步發展之可能性）、是否適合在學術期刊發表或申請專利、主要發現（簡要敘述成果是否具有政策應用參考價值及具影響公共利益之重大發現）或其他有關價值等，作一綜合評估。

1. 請就研究內容與原計畫相符程度、達成預期目標情況作一綜合評估
   ■達成目標
   □未達成目標（請說明，以100字為限）
   　□實驗失敗
   　□因故實驗中斷
   　□其他原因
   說明：

2. 研究成果在學術期刊發表或申請專利等情形（請於其他欄註明專利及技轉之證號、合約、申請及洽談等詳細資訊）
   論文：□已發表　■未發表之文稿　□撰寫中　□無
   專利：□已獲得　□申請中　■無
   技轉：□已技轉　□洽談中　■無
   其他：（以200字為限）

3. 請依學術成就、技術創新、社會影響等方面，評估研究成果之學術或應用價值（簡要敘述成果所代表之意義、價值、影響或進一步發展之可能性，以500字為限）
   近年來3D列印已成為多種生醫材料開發研究的技術，本實驗室藉由開發出的含Sr的矽酸鈣骨粉，結合3D列印技術已開發出多孔支架，除了可以有效促進細胞生長，目前從動物實驗結果中也可得知能夠有效地促進骨組織的修復及再生，有機會在未來作為骨組織工程用的材料之一。

4. 主要發現
   本研究具有政策應用參考價值：■否　□是，建議提供機關
   （勾選「是」者，請列舉建議可提供施政參考之業務主管機關）
   本研究具影響公共利益之重大發現：□否　□是
   說明：（以150字為限）